Apply Optimization Algorithm to Develop Parallel Navigation Guidance Law

Y.-W. Chen

**Department of Mechanical Engineering, Air Force Institute of Technology, Taiwan R.O.C.*
(e-mail: chenyiwei530@yahoo.com.tw).

Abstract: The proposed missile parallel navigation guidance law utilizes the current dynamics of both the target and the missile to compute the line-of-sight rate and applies missile acceleration control command equations within the framework of proportional navigation guidance to control the missile's flight route. In this study, particle swarm optimization is used to continuously optimize the navigation constants and update the missile acceleration control commands, where the line-of-sight rate is defined as the fitness function of particle swarm optimization. The missile moves toward the target in parallel navigation guidance mode when the computed value of the fitness function approaches zero during the optimization process. There are three different pursuit-evasion scenarios in a three-dimensional space in the simulation experiments, where the target information includes noise disturbances to better simulate real target-interceptor engagement conditions. The simulation results prove that the proposed guidance theory is highly effective in intercepting maneuvering targets with high G-force, whereas proportional navigation guidance cannot achieve this effectively. Furthermore, a missile guidance algorithm using particle swarm optimization has been reproduced, which serves as the main motivation for developing the proposed guidance method in this study. The experiments demonstrate that the PSO-based missile guidance algorithm may produce oscillations in the control commands during pursuit-evasion, which could affect both the guidance performance and structural integrity of the missile. However, the proposed guidance method in this study not only mitigates these oscillations but also achieves better overall guidance performance.

Keywords: Missile; Guidance; Optimization; Parallel navigation guidance.

1. INTRODUCTION

The capabilities of modern aircraft have been continuously upgraded due to advancements in aerospace technology, which impact the interception ability of missiles. To address this issue, it is essential to enhance the performance of missile guidance laws. Artificial intelligence (AI) has been widely applied to solve problems related to nonlinear systems and optimization technology. Missile guidance algorithms also utilize AI to achieve breakthroughs in guidance capability.

The crucial aspect of missile guidance development is to minimize the miss distance between the target and the missile while reducing the phenomenon of acceleration saturation in the missile. Therefore, the miss distance and missile acceleration during the pursuit-evasion process serve as important indicators for evaluating the effectiveness of a missile guidance law. Traditional missile guidance laws may be incapable of intercepting fast aircraft with high agility. The widely used proportional navigation guidance (PNG) law, which has been extensively applied in warfare, utilizes the line-of-sight (LOS) rate and missile velocity to generate missile control commands. PNG benefits from a simple theoretical model that can be easily integrated into missile guidance control systems. PNG is effective for intercepting a target moving in a straight-line, head-on, or pursuit trajectory. Besides, generalized proportional navigation guidance (GPNG) and realistic true proportional navigation guidance (RTPNG) are extended modes of PNG (Wang and Liao, 2024). With the increasing agility of aircraft, PNG gradually adjusts the flight route in the initial stage and increases the missile's acceleration control commands in the final stage, significantly altering the missile's dynamics and making acceleration saturation more likely. The above condition can easily lead to a large miss distance. An improved version of PNG, such as the augmented proportional navigation guidance (APNG) law, has been proposed to enhance guidance performance. APNG primarily incorporates the target acceleration term into the missile's guidance command to reduce the impact of target maneuvers. However, obtaining accurate target acceleration data is challenging. Lin et al. use the predicted interception point to compute the steering angle, which is then applied to generate the missile's guidance command. This method achieves better interception performance than PNG; however, it requires the proper selection of navigation constants beforehand (Lin et al., 2010). Nonlinear control theory has been utilized to deal with target-interceptor problems through techniques such as backstepping control, adaptive control, and sliding mode control. However, missile guidance techniques based on nonlinear control theory rely on complex controller designs or detailed target model information. These operational constraints make real-time target-interceptor engagement challenging (Chen, 2022).

AI has been developed for several decades and has been applied to various research fields, such as optimization problems and control systems. It has been proven that AI can effectively solve complex nonlinear problems and achieve satisfactory research results. Therefore, the development of missile guidance algorithms based on AI is both intriguing and widely studied. Balakrishnan et al. utilized neural networks to develop an optimized missile homing guidance law for target interception. The improved versions, incorporating the concept of adaptive critics capable of online learning, can be used to intercept targets flying in a linear or approximately linear trajectory (Steck and Balakrishnan, 1994; Balakrishnan and Biega, 1995; Dalton and Balakrishnan, 1996). Song et al. utilized neural networks to propose midcourse guidance algorithms from 1996 to 2002. The first was a feedforward neural network guidance law with real-time computing capability. Subsequently, a calibration-based approach for the midcourse stage and a feedback-based approach for the homing stage, both based on a neural network framework, were developed to intercept targets or ballistic missiles in three-dimensional space (Song and Tahk, 1998; Song and Tahk, 1999; Song and Tahk, 2001; Song and Tahk, 2002). Mishra et al. used both the acceleration control command based on the PNG scheme and fuzzy logic theory to infer the real-time acceleration control command in order to develop a fuzzy missile homing guidance law (Mishra et al., 1994). Omar and Abido proposed an integrated fuzzy guidance law combined with the Strength Pareto Evolutionary Algorithm. This algorithm is mainly composed of three fuzzy controllers, which can be applied to three different guidance stages during pursuit-evasion (Omar and Abido, 2010). The capability of a guidance law developed based on a neural network scheme would be influenced by a variety of parameters and the training process, and the application of fuzzy logic theory increases the storage burden on computers. In addition, genetic algorithm has been applied to develop missile guidance laws, but they require consideration of coding issues, parameter design, and the evolution process (Qi et al., 2003; Yang et al., 2005). Kung and Chen proposed a feasible guidance algorithm based on particle swarm optimization (PSO), where the application of fitness function guides the missile toward the current position of the target. However, this method can easily produce large missile acceleration control commands during the pursuit-evasion process, especially when intercepting a maneuvering target (Kung and Chen, 2013). Chen et al. proposed an improved PSO guidance law in 2016, which applied PSO to optimize the missile acceleration control commands, with the LOS rate used to design the fitness function. The missile's guidance mode was developed based on the theory of parallel navigation guidance (PN), and its interception performance are satisfied (Chen et al., 2016).

PNG has the characteristics of a simple theoretical model and has been widely applied to missile guidance control systems due to its ease of implementation. However, PNG may be ineffective in intercepting highly maneuvering targets. Most missile guidance algorithms developed based on AI are difficult to apply in practice due to complex computations and storage burdens. PN is derived from a simple logical concept. It assumes that when two objects gradually get closer to each other, they will eventually intersect at a specific moment if the angle between the line-of-sight (LOS) and the reference horizontal line in inertial space remains constant. Therefore, the missile will ultimately be able to intercept the target based on this concept. The advantages of PN include a straight trajectory, low energy consumption, and the capability for omnidirectional attacks. However, its disadvantages include the requirement for precise measurements of the missile's and target's velocity and heading angle at every moment. Additionally, factors such as launch deviations and the effects of external disturbances make this method difficult to implement in practice. In this study, the proposed method is developed based on the concept of PN and the application of two lateral acceleration control command equations within the framework of PNG. A guidance theory approximating the PN mode can be developed by leveraging the advantages of PSO, such as its fast convergence speed, minimal parameter requirements, and resistance to local optimum.

2. MATHMATICAL MODELS OF TARGET AND MISSILE DYNAMICS

The target is assumed to be a point mass to establish the mathematical model of target dynamics, which can be used to simulate the tactical flight route controlled by the pilot (Fig. 1). The following mathematical equations describe the motion state of the target in a three-dimensional space, and are expressed in the inertial coordinate system (Chen, 2022; Chen et al, 2021; Sun et al., 2008).

$$x_t' = v_t \cos\gamma_t \cos\theta_t \tag{1}$$

$$y_t' = v_t \cos\gamma_t \sin\theta_t \tag{2}$$

$$z_t' = v_t \sin\gamma_t \tag{3}$$

$$v_t' = g\left(n_x - \sin\gamma_t\right) \tag{4}$$

$$\gamma_t' = \frac{g}{v_t}\left(n_z \cos\phi - \cos\gamma_t\right) \tag{5}$$

$$\theta_t' = \frac{g n_z \sin\phi}{v_t \cos\gamma_t} \tag{6}$$

The target's flight route can be controlled by changing the control commands (n_x , n_z , ϕ). However, the target's motion state does not instantaneously follow these commands due to inertia. To address this issue, the following dynamic time delay models are applied.

$$n_x = \frac{n_{xc}}{1 + s\tau_{tx}} \tag{7}$$

$$n_z = \frac{n_{zc}}{1 + s\tau_{tz}} \tag{8}$$

$$\phi = \frac{\omega_n^2}{s^2 + 2\omega_n \xi s + \omega_n^2} \times \phi_c \tag{9}$$

x_t, y_t, z_t : Target position in x, y, z direction.

x_t', y_t', z_t' : Target velocity in x, y, z direction.

v_t : Target velocity.

γ_t : Pitch angle.

θ_t : Yaw angle.

n_x : Load factor along the target velocity direction.

n_z : Load factor along the pitch direction.

ϕ : Load factor of rolling angle.

n_{xc}, n_{zc}, ϕ_c : Control commands.

τ_{tx}, τ_{tz} : Time delay constants.

ω_n : Natural frequency.

ξ : Damping ratio.

g : Gravitational acceleration.

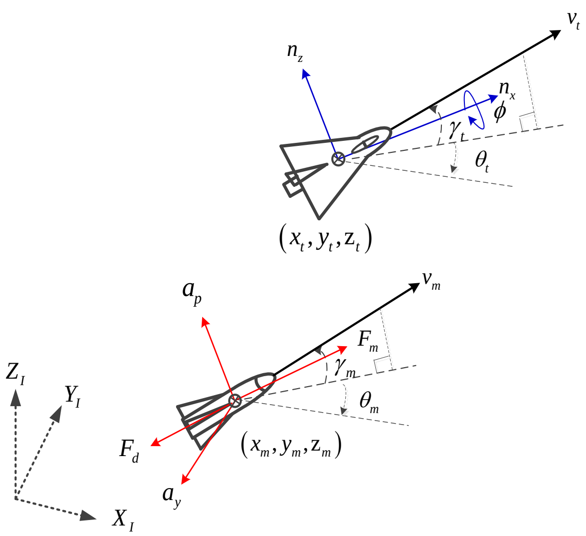

Fig. 1. Mathematical models of target and missile dynamics.

The missile is assumed to be a point mass to develop the mathematical model of missile dynamics, which can be used to simulate the interceptor (Fig. 1). The following mathematical equations describe the missile's motion state in a three-dimensional space and are expressed in the inertial coordinate system (Chen, 2022; Chen et al, 2021; Fumiaki, 1993).

$$x_m' = v_m \cos\gamma_m \cos\theta_m \tag{10}$$

$$y_m' = v_m \cos\gamma_m \sin\theta_m \tag{11}$$

$$z_m' = v_m \sin\gamma_m \tag{12}$$

$$v_m' = \frac{F_m - F_d}{M_m} - g \sin\gamma_m \tag{13}$$

$$\gamma_m' = \frac{a_p - g\cos\gamma_m}{v_m} \tag{14}$$

$$\theta_m' = \frac{a_y}{v_m \cos\gamma_m} \tag{15}$$

The missile flight route can be controlled by changing the lateral acceleration (a_p , a_y), but the missile motion state does not instantaneously follow the lateral acceleration control commands due to inertia. Therefore, the following dynamic time delay models are applied to address this problem.

$$a_p' = \frac{C_p - a_p}{\tau_m} \tag{16}$$

$$a_y' = \frac{C_y - a_y}{\tau_m} \tag{17}$$

F_m , M_m and F_d in equation (13) can be computed as follows.

$$F_m = \begin{cases} F_m, & t \le t_B \\ 0, & t > t_B \end{cases} \tag{18}$$

$$M_m = \begin{cases} M_{mi} - M't, & t \le t_B \\ M_{mf}, & t > t_B \end{cases} \tag{19}$$

$$F_d = k_1 v_m^2 + k_2 \frac{C_p^2 + C_y^2}{v_m^2} \tag{20}$$

x_m, y_m, z_m : Missile position in x, y, z direction.

x_m', y_m', z_m' : Missile velocity in x, y, z direction.

v_m : Missile velocity.

γ_m : Pitch angle.

θ_m : Yaw angle.

a_p : Lateral acceleration along the pitch direction.

a_y : Lateral acceleration along the yaw direction.

C_p : Lateral acceleration control command along the pitch direction.

C_y : Lateral acceleration control command along the yaw direction.

τ_m : Time delay constant.

F_m : Thrust force.

M_m : Missile mass.

M_{mi} : Missile mass at initial stage.

M_{mf} : Missile mass at final stage.

M' : Combustion rate of missile rocket propulsion.

t_B : Working time of thrust force.

F_d : Drag force.

k_1, k_2 : Drag force coefficients.

3. PARALLEL NAVIGATION GUIDANCE ALGORITHM

3.1 PN and PNG

According to PN algorithm concept, the missile will ultimately be able to intercept the target if the LOS angle defined as the angle between the LOS and the reference horizontal line in inertial space remains constant during the pursuit-evasion process (Siouris, 2004). PN mode is illustrated in Fig. 2 and ψ, σ is defined as LOS angle. The missile flight route in PN algorithm is characterized by low curvature compared to most of missile guidance laws, which leads to efficient target interception. However, it is difficult to implement this method because PN relies heavily on precise measurements of the missile's and target's velocity and heading angle at every moment. Moreover, if the target performs abrupt or highly nonlinear maneuvers, the missile may struggle to adapt while maintaining a parallel trajectory. According to the concept of PN algorithm, it would be feasible to implement PN algorithm if LOS rate can be approximated to zero ($\psi' = 0, \sigma' = 0$).

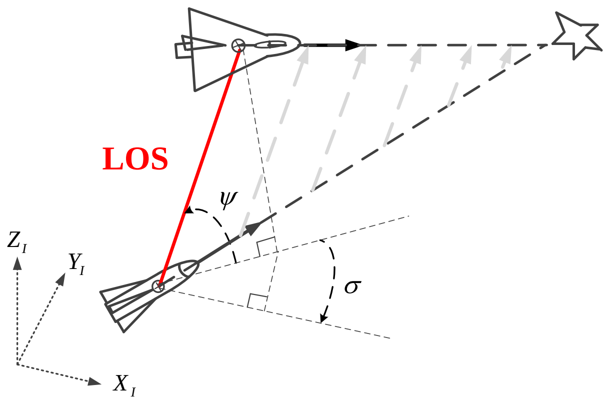

Fig. 2. Illustration of PN mode.

PNG is a mature and widely used guidance algorithm applied in missile guidance systems. PNG primarily utilizes the LOS rate and missile velocity to generate the guidance control commands. In PNG algorithm, the lateral acceleration control commands of missile in a three-dimensional space can be expressed as follows:

$$C_p = N_p v_m \psi' + g\cos\gamma_m \tag{21}$$

$$C_y = N_y v_m \sigma' \tag{22}$$

N_p, N_y : Navigation constants.

ψ, σ : LOS angle.

3.2 Particle Swarm Optimization (PSO)

Particle Swarm Optimization (PSO) was proposed by Eberhart and Kennedy. PSO algorithm is developed based on the imitation of birds foraging behaviour (Eberhart and Kennedy, 1995). In PSO algorithm, a group of random particles is generated and each particle is defined as a solution in the problem space. These particles search for the optimal value to solve the proposed problem and record the path at each step during the evolution process. The best position found by each particle is defined as the local optimal solution. These particles can deliver messages to each other to find the best way to solve the problem, where the best particle in this group is defined as the global optimal solution. The operation of PSO algorithm can be briefly described in the following steps:

1. Generate a group of random particles and each particle can be defined as a possible solution.

2. Apply these possible solutions to the proposed problem.

3. Define the fitness function and compute the fitness value for each particle.

4. Update the local optimal solution and the global optimal solution.

5. Update each particle’s position and velocity as shown in Eq. (23) and Eq. (24).

6. Set a threshold to determine the end of the optimization process and repeat the evolution steps until the threshold is met.

$$\begin{aligned} V^i(j+1) &= W_e V^i(j) + L_1 R_1 \left(Pbest^i(j) - X^i(j)\right) \\ &+ L_2 R_2 \left(Gbest_g(j) - X^i(j)\right) \end{aligned} \tag{23}$$

$$X^i(j+1) = X^i(j) + V^i(j+1) \tag{24}$$

i : Serial number of particle.

j : Iteration time.

V^i : Particle velocity.

X^i : Particle position.

W_e : Inertial weight.

R_1, R_2 : Random numbers in the interval (0, 1).

L_1, L_2 : Learning factors.

$Pbest^i$: Local optimal solution.

$Gbest_g$: Global optimal solution.

3.3 PROPOSED MISSILE GUIDANCE LAW

This study is developed based on the concept of PN. The author utilizes two lateral acceleration control command equations of PNG to control the missile's flight route, where PSO is applied to optimize the navigation constants and update the missile's acceleration control commands. Additionally, the LOS rate is defined as fitness function of PSO so that the missile can intercept the target in PN mode when the computed value of fitness function approaches zero during the optimization process. Fig. 3 presents the flow chart of the proposed PN algorithm and the operation steps are explained in detail as follows:

(1) Initial settings:

A. Define PSO parameters such as particle quantity, inertia weight, learning factors, maximum evolution times, and threshold.

B. Initialize the parameters of dynamic equations for the missile and the target, and design the target's flight route by adjusting the control commands.

C. Apply Runge Kutta method to conduct simulation experiments of three-dimensional target-interceptor engagement.

(2) Computing LOS rate:

Define (x_r, y_r, z_r) as the distance between the target and the missile in X-axis, Y-axis, Z-axis of inertial coordinate:

$$x_r = x_t - x_m;$$
$$y_r = y_t - y_m;$$
$$z_r = z_t - z_m$$

Define (x_r', y_r', z_r') as the velocity difference between the target and the missile in X-axis, Y-axis, Z-axis of inertial coordinate:

$$x_r' = v_t \cos\gamma_t \cos\theta_t - v_m \cos\gamma_m \cos\theta_m;$$
$$y_r' = v_t \cos\gamma_t \sin\theta_t - v_m \cos\gamma_m \sin\theta_m;$$
$$z_r' = v_t \sin\gamma_t - v_m \sin\gamma_m$$

Then LOS rate can be computed by the following equations:

$$\sigma' = \frac{(x_r y_r' - x_r' y_r)}{(x_r^2 + y_r^2)} \tag{25}$$

$$\psi' = \frac{z_r'\left(x_r^2 + y_r^2\right) - z_r\left(x_r x_r' + y_r y_r'\right)}{\sqrt{x_r^2 + y_r^2}\left(x_r^2 + y_r^2 + z_r^2\right)} \tag{26}$$

(3) Define the navigation constants of PNG as a two-dimensional particle and the position of each particle in PSO algorithm is defined as $X_i = \left[N_p^i \quad N_y^i\right]^T$, $1 \le i \le Q$. Q is the total number of particles, which is equal to the number of solutions. In this step, randomize the navigation constants within a reasonable interval.

(4) Use LOS rate and N_p^i, N_y^i to compute the possible lateral acceleration control commands of missile (C_p^i, C_y^i) by Eq. (21) and Eq. (22):

(5) Apply C_p^i, C_y^i to the missile dynamic model to obtain the possible position of missile at the next time interval $\left(x_m^i(t+\Delta t), y_m^i(t+\Delta t), z_m^i(t+\Delta t)\right)$.

(6) Compute LOS rate in accordance with the outcome of step 5.

(7) The definition of fitness function in this study refers to the concept of referenced study (Chen et al., 2016) as follows:

$$\Phi = \sqrt{\left[\left(\sigma^i\right)'\right]^2 + \left[\left(\psi^i\right)'\right]^2} \tag{27}$$

(8) Compute the fitness value of each particle and the minimal fitness value is defined as the local optimal solution during the evolution process. The particle with the lowest fitness value in the group is defined as the global optimal solution.

(9) Update the particle's position and velocity.

(10) Define the deviation as the threshold and repeat the evolution process from step (4) to step (9) to compute the optimal navigation constants (N_p, N_y) until the threshold is satisfied.

(11) Apply N_p, N_y to compute the optimal control commands (C_p, C_y) that are restricted within the maximum acceleration ($a_{\max}$) due to consideration of missile's body structure and dynamic capability.

(12) Update the missile's position.

(13) Repeat the process from step (2) to step (12) and design the ending rules to stop the operation according to the relative distance (R_t) between the missile and the target, and working time of missile thrust force (t_B). The

calculation of the proposed method will end if $R_t > R_{t-1}$ or $t > t_B$ and that obtain the miss distance and interception time.

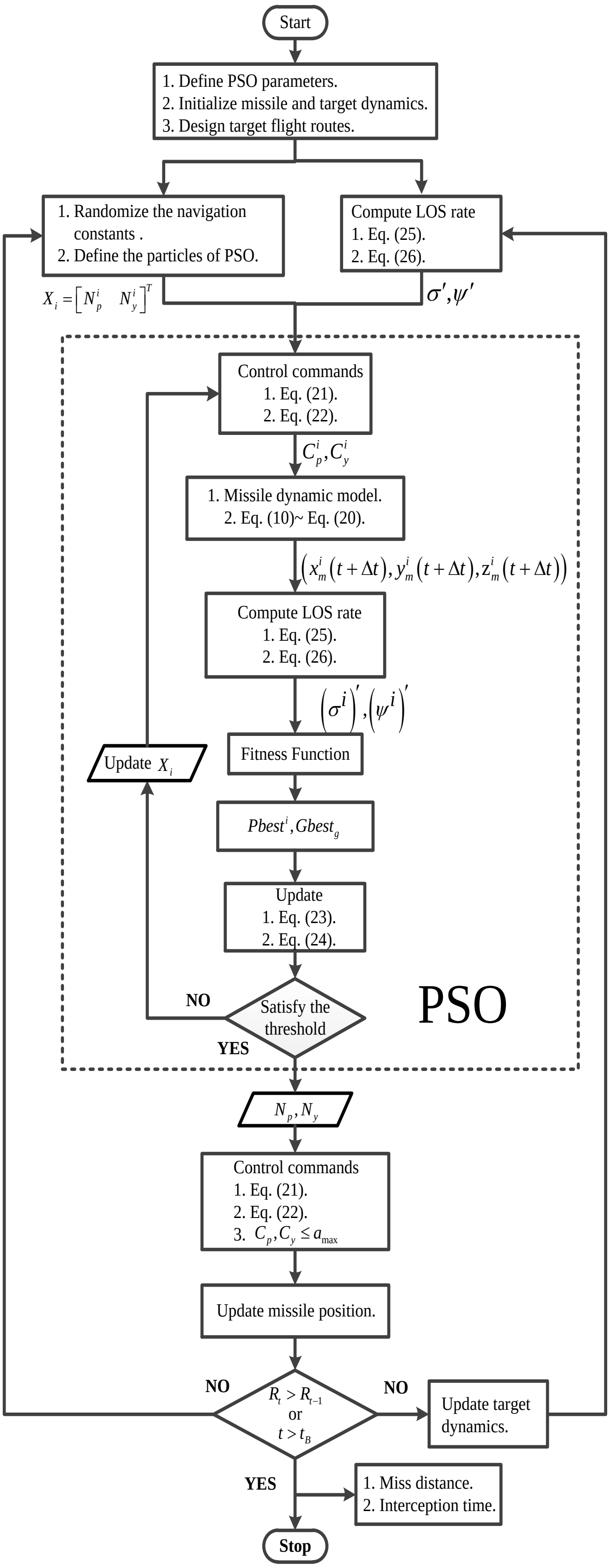

Fig. 3. Flow chart of the proposed PN algorithm.

4. RESULTS AND DISCUSSION

The optimization algorithms have been applied to design the missile guidance law in the past decades. Chen et al. have successfully applied PSO to optimize the acceleration control commands of missile to design the missile guidance law. Furthermore, the missile guidance mode is similar to PN theory due to the core design of PSO fitness function and the guidance performance is extraordinary (Chen et al., 2016).

Three different simulation scenarios of target-interceptor engagement are conducted to verify the effectiveness of the proposed PN algorithm using PSO (PN-PSO). Additionally, the conventional PNG is used for comparison with PN-PSO, and the author also reproduces the improved PSO guidance law (IPSOG) in 2016 (Chen et al., 2016) to analyze the difference in guidance ability between PN-PSO and IPSOG. The inertial coordinate system is used to illustrate the pursuit-evasion scenarios of target-interceptor in the simulation experiments. The measurement data of the target state contains white Gaussian noise, and signal-to-noise ratio is set to 50 to approximate the real engagement environment. The missile's weight and thrust would change over time. Besides, noise disturbances and optimization process of PSO may lead to slight deviation in experimental results under the same simulation scenarios. Therefore, each of the three different guidance algorithms in this study is executed by 10 times per scenario to validate the guidance performance.

Table 1 is the initial condition for the engagement of target-interceptor and Table 2 is the design of PSO parameters in simulation experiments. In addition, the parameters for mathematical models of target and missile dynamics are designed as follows (Chen, 2022): time delay constants $\tau_{tx}, \tau_{tz}, \tau_m = 0.1$, natural frequency $\omega_n = 10$ (Hz), damping ratio $\xi = 0.7$, drag force coefficients $k_1 = 0.001$, $k_2 = 1$, missile mass $M_{mi} = 165$ (kg), $M_{mf} = 125$ (kg), $M' = 2.66$ (kg/sec), thrust force $F_m = 5880$ (N), working time of thrust force $t_B = 15$ (sec), sampling time $\Delta t = 0.02$ (sec), The navigation constants in PNG are 3. The maximum lateral acceleration control commands of missile are 30 (g).

Table 1. Initial condition for the engagement of target-interceptor.

Scenario		Position (m)	Velocity (m/sec)	Pitch (degree)	Yaw (degree)
I	Target	(5000,5000,3000)	200	0	0
	Missile	(1000,1000,1000)	600	0	0
II	Target	(5000,4000,3000)	300	30	15
	Missile	(1000,1000,1000)	600	0	0
III	Target	(5000,5000,5000)	250	15	45
	Missile	(1000,1000,1000)	600	30	30

Table 2. Design of PSO parameters.

Maximal evolution times	Particle amount	Inertia weight	Learning factors	Threshold
500	200	0.5	$f_1 = 1, f_2 = 1$	0.01

Scenario I: Table 3 shows the interception performance of missile using PN-PSO, IPSOG and PNG against the target moving along a nearly straight-line route. Both PN-PSO and IPSOG demonstrate superior interception capabilities, characterized by shorter miss distance and interception time compared with PNG. Fig. 4 illustrates the interception trajectories of missile using PN-PSO, IPSOG, and PNG against a nearly straight-line target. The flight trajectories of IPSOG and PN-PSO are smooth and similar, while PNG features a large curvature and a long trajectory, which explain why PNG requires more time to intercept the target. Fig. 5-7 show the variation of missile control commands over time for three different guidance algorithms. The pitch and yaw control commands of missile in IPSOG exhibit significant oscillations during the target pursuit process, indicating that the missile continuously and drastically changes its motion state. For PN-PSO, the pitch and yaw control commands of missile show large variations during the first 2 seconds. Between the 2nd and 7th seconds, the control command values remain small and stable. After the 7th second, as the missile gradually closes the distance to the target, measurement noise significantly affects the missile's control commands, resulting in large variations within a short period of time. For PNG, the pitch and yaw control commands of missile remain stable during the first 8 seconds. After the 9th second, as the missile gets closer to the target, it is similarly affected by measurement noise, causing significant variations in the missile's control commands.

Table 3. Interception performance of missile using PN-PSO, IPSOG and PNG against the target moving along a nearly straight-line route in Scenario II.

No.	Miss Distance (m)			Interception Time (sec)		
	PN-PSO	IPSOG	PNG	PN-PSO	IPSOG	PNG
1	2.79	4.96	7.70	9.94	9.92	10.18
2	6.41	9.09	10.05	9.94	9.92	10.18
3	6.62	4.13	13.37	9.94	9.92	10.18
4	5.85	5.38	11.92	9.94	9.92	10.18
5	2.23	4.39	10.54	9.94	9.92	10.18
6	7.98	8.15	10.34	9.94	9.92	10.18
7	7.72	6.84	10.51	9.94	9.92	10.18
8	2.89	5.69	7.37	9.94	9.92	10.18
9	5.68	3.33	7.46	9.94	9.92	10.18
10	3.02	4.41	9.92	9.94	9.92	10.18

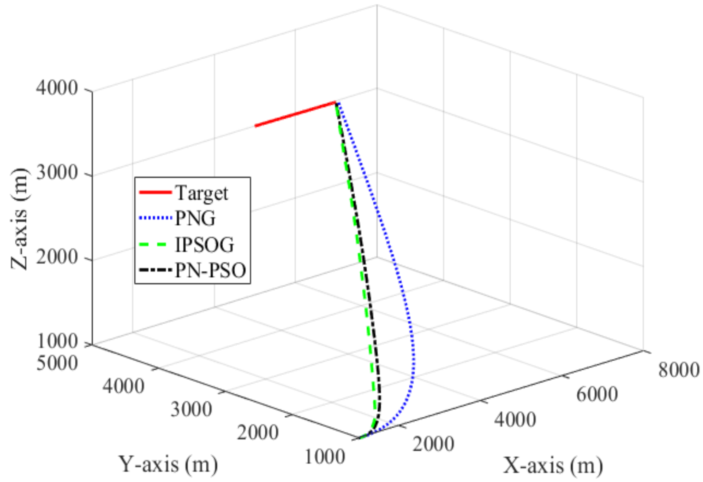

Fig. 4. Interception trajectories of missile using PN-PSO, IPSOG, and PNG against a nearly straight-line target in Scenario I.

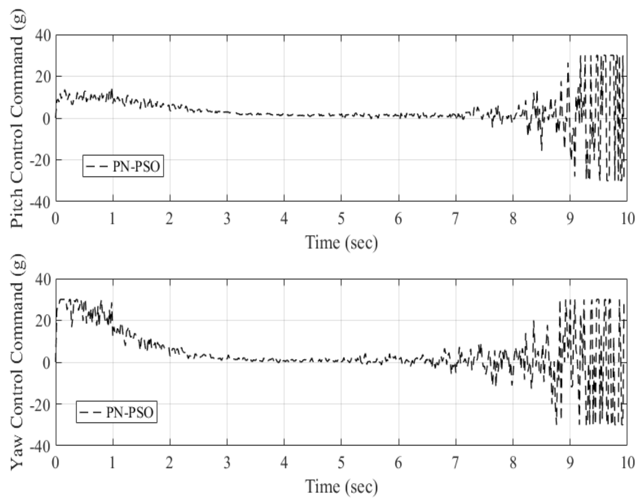

Fig. 5. Variation of missile control commands over time for PN-PSO in Scenario I.

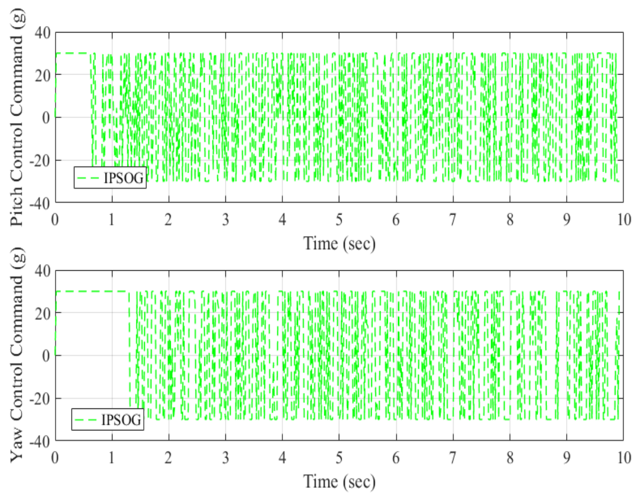

Fig. 6. Variation of missile control commands over time for IPSOG in Scenario I.

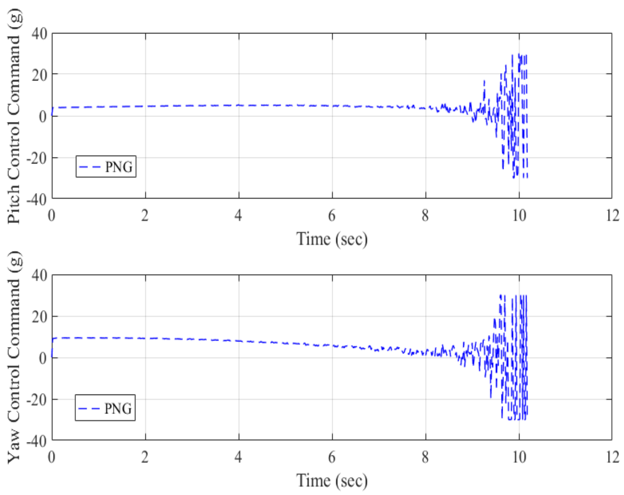

Fig. 7. Variation of missile control commands over time for PNG in Scenario I.

Scenario II: Table 4 shows the interception performance of missile using PN-PSO, IPSOG and PNG against the target with big G-force turn. The miss distance of PNG is at least 11 m, and the interception time is relatively long. IPSOG has the shortest interception time among the three guidance algorithms and a shorter miss distance than PNG, but in terms of miss distance, PN-PSO demonstrates superior interception capability compared to IPSOG. Fig. 8 illustrates the interception trajectories of missile using PN-PSO, IPSOG, and PNG against a big G-force turning target. The flight trajectories of PN-PSO and IPSOG are smooth with minimal variation, whereas PNG exhibits significant trajectory variation and a longer path. The limitation of PNG guidance capability becomes evident when dealing with big G-force turning targets.

Table 4. Interception performance of missile using PN-PSO, IPSOG and PNG against the target with big G-force turn in Scenario II.

No.	Miss Distance (m)			Interception Time (sec)		
	PN-PSO	IPSOG	PNG	PN-PSO	IPSOG	PNG
1	8.57	10.06	17.93	9.16	9.12	9.64
2	2.36	8.67	15.11	9.16	9.12	9.64
3	4.27	8.23	11.17	9.16	9.12	9.64
4	9.02	9.02	14.97	9.16	9.12	9.64
5	9.34	10.59	11.16	9.16	9.12	9.64
6	8.74	8.79	12.14	9.16	9.12	9.64
7	6.28	9.18	13.98	9.16	9.12	9.64
8	10.12	9.64	11.85	9.16	9.12	9.64
9	9.31	11.50	12.87	9.16	9.12	9.64
10	4.49	9.97	16.92	9.16	9.12	9.64

Fig. 9-11 show the variation of missile control commands over time for three different guidance algorithms. The pitch and yaw control commands of missile in IPSOG exhibit significant oscillations during the target pursuit process. For PN-PSO, the pitch and yaw control commands of missile respond to drastic changes in the target motion state, reaching close to the maximum value of 30 g within the first 0.5 seconds. Between the 2nd and 7th seconds, the control command values remain small and relatively stable. After the 7th second, measurement noise significantly affects the missile's control commands to cause large fluctuations as the missile progressively approaches the target. The variation trend of the pitch and yaw control commands for PNG is similar to that observed in Scenario I.

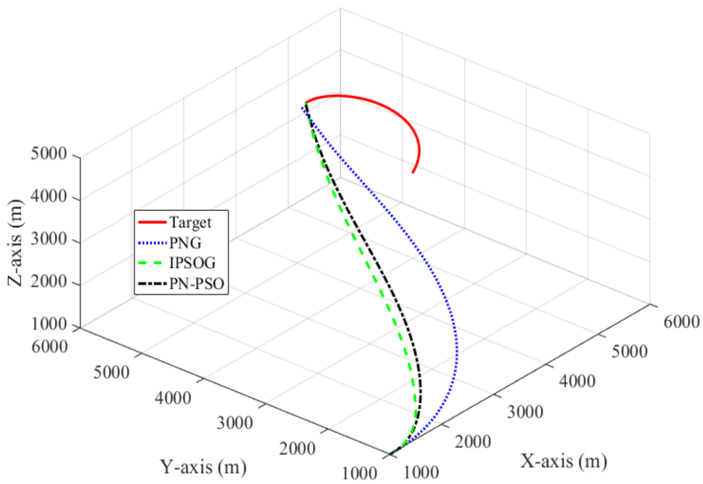

Fig. 8. Interception trajectories of missile using PN-PSO, IPSOG, and PNG against a big G-force turning target in Scenario II.

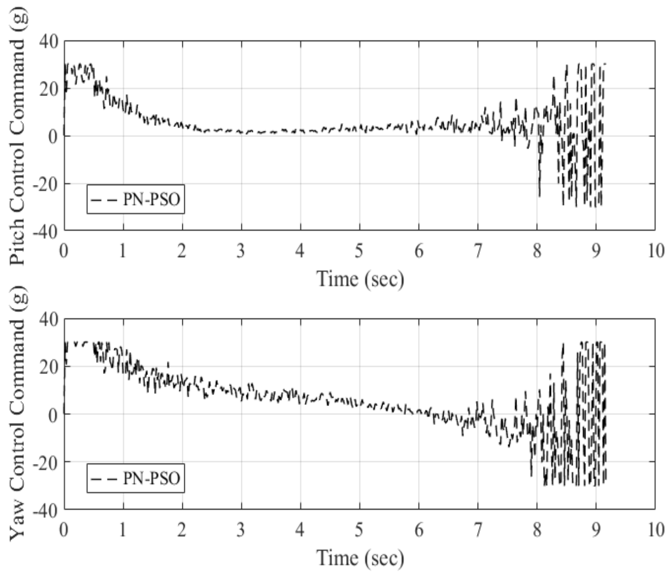

Fig. 9. Variation of missile control commands over time for PN-PSO in Scenario II.

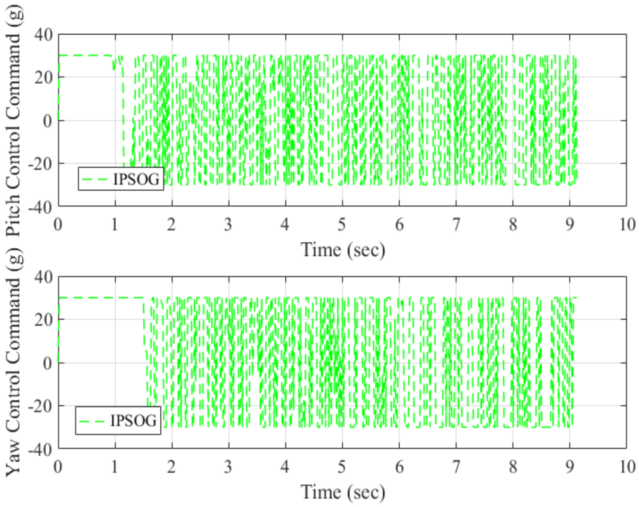

Fig. 10. Variation of missile control commands over time for IPSOG in Scenario II.

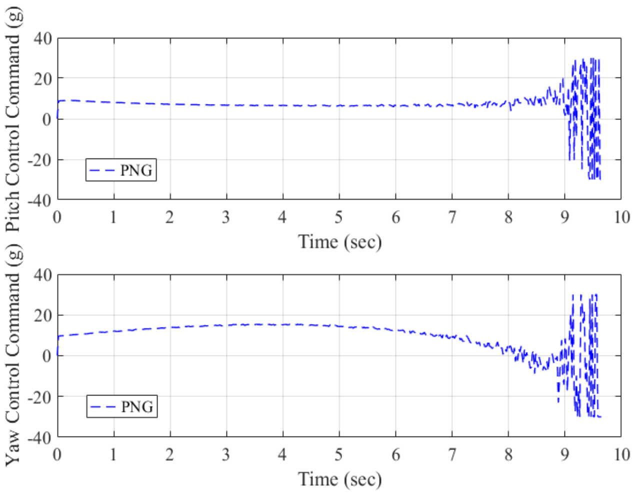

Fig. 11. Variation of missile control commands over time for PNG in Scenario II.

Scenario III: Table 5 shows the interception performance of missiles using PN-PSO, IPSOG, and PNG against a highly maneuverable evasive target. The interception time for the three guidance algorithms are nearly identical. In terms of miss distance performance, PN-PSO performs the best, followed by IPSOG, while PNG performs the worst. However, IPSOG shows the worst miss distance performance in the 2nd, 5th, and 6th experiments. Fig. 12 illustrates the interception trajectories of missile using PN-PSO, IPSOG, and PNG against a highly maneuverable evasive target. The missile flight trajectories of three guidance algorithms exhibit significant changes in response to the high-maneuver behaviors of the target. Fig. 13-15 show the variation of missile control commands over time for three different guidance algorithms. Similar to the situations in Scenarios I and II, the pitch and yaw control commands of missile in IPSOG exhibit significant oscillations during the pursuit-evasion process. The curve variations of the pitch control commands for PN-PSO and PNG are similar and relatively stable. However, the changes in yaw control commands for both are very obvious, corresponding to the target's S-curve maneuver behavior. As the missile gradually approaches the target, measurement noise significantly affects the missile control commands, causing large fluctuations.

Table 5. Interception performance of missiles using PN-PSO, IPSOG, and PNG against a highly maneuverable evasive target in Scenario III.

No.	Miss Distance (m)			Interception Time (sec)		
	PN-PSO	IPSOG	PNG	PN-PSO	IPSOG	PNG
1	5.91	9.06	10.92	11.56	11.56	11.56
2	5.22	10.47	8.69	11.56	11.56	11.56
3	10.42	11.77	12.24	11.56	11.56	11.56
4	4.41	8.75	9.33	11.56	11.56	11.56
5	4.16	9.72	7.67	11.56	11.54	11.54
6	11.26	12.74	12.49	11.56	11.56	11.56
7	11.23	11.01	12.28	11.56	11.56	11.56
8	6.25	9.85	10.40	11.56	11.56	11.54
9	11.19	12.99	13.81	11.56	11.56	11.56
10	5.24	10.98	11.17	11.56	11.56	11.56

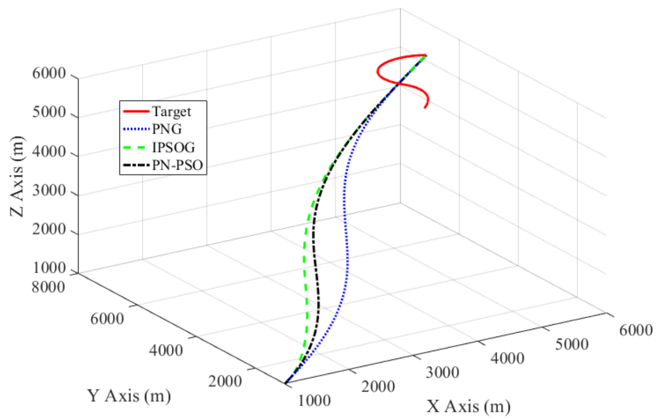

Fig. 12. Interception trajectories of missile using PN-PSO, IPSOG, and PNG against a highly maneuverable evasive target in Scenario III.

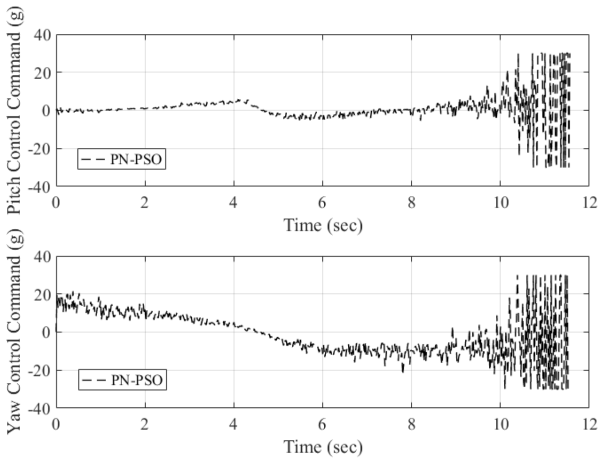

Fig. 13. Variation of missile control commands over time for PN-PSO in Scenario III.

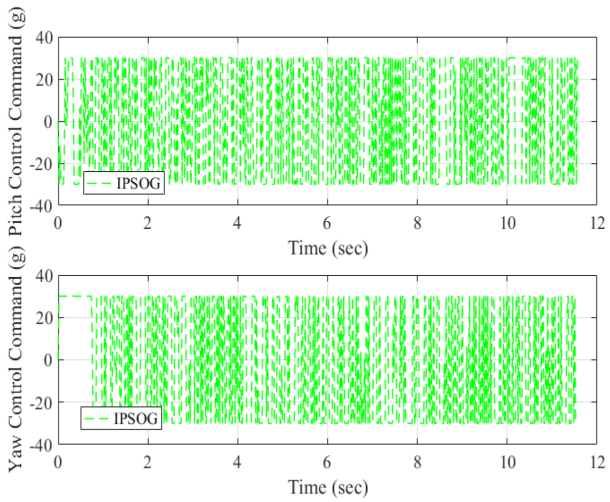

Fig. 14. Variation of missile control commands over time for IPSOG in Scenario III.

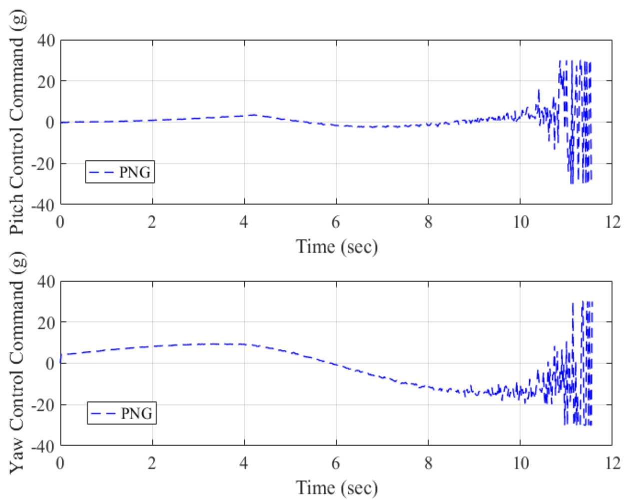

Fig. 15. Variation of missile control commands over time for PNG in Scenario III.

The core of IPSOG algorithm is the application of PSO to design and optimize the missile's lateral acceleration control commands with the LOS rate defined as the fitness function. The missile can be guided toward the target in PN mode when the computed value of fitness function approaches zero during the optimization process. The proposed PN-PSO algorithm, on the other hand, utilizes two lateral acceleration control command equations based on PNG framework. It applies PSO to update the navigation constants to optimize the missile's acceleration control commands. Similarly, the definition of fitness function follows the concept of IPSOG so that the missile can fly towards the target in a PN mode. According to the simulation results of the above scenarios, the missile flight trajectories of IPSOG and PN-PSO are very similar. In Scenario I, both IPSOG and PN-PSO demonstrate excellent interception performance, while in Scenario II and III, the interception capability of PN-PSO is better than IPSOG. In Scenario III, IPSOG even shows a larger miss distance than PNG. Based on the variation in missile control commands over time for IPSOG in three different scenarios, it is evident that the missile control commands cause severe oscillation during the pursuit-evasion process. This indicates that the missile undergoes continuous and significant changes in its motion state, which could potentially affect both its guidance performance and structural integrity. This oscillation phenomenon mainly stems from the parameter design of the missile control commands during the PSO optimization process. The guidance capability of PNG appears inadequate to the target with big G-force turn or highly maneuvers. The simulation experiments in this study were conducted under conditions where the measurement data of target contained noise. The interception performance of three different guidance algorithms could be further improved if the filtering techniques were applied.

In PSO algorithm, the number of particles is related to the complexity of problem. In general, the complex mathematical problems require a larger number of particles. The inertia weight affects the exploration capability and the convergence speed of optimization, while the learning factors influence the balance between local and global optimum solutions. The author refers to the design of PSO parameters in this referenced study (Chen, 2022) to conduct the simulation experiments.

5. CONCLUSIONS

The proposed missile guidance algorithm is developed based on the concept of PN. It computes the LOS rate according to the current motion states of both the target and the missile, and applies PSO to optimize the navigation constants, thereby continuously update the missile's acceleration control commands. In this approach, the LOS rate is defined as the fitness function and the missile moves toward the target in PN mode as the computed value of fitness function approaches zero during the optimization process.

Simulation experiments have shown that the missile flight trajectories of the proposed method are smooth and exhibit better interception performance compared to PNG during the pursuit-evasion scenarios. Additionally, this study reproduces a PSO-based missile guidance algorithm in which the missile moves to intercept the target in PN mode. In comparison, the proposed method in this paper demonstrates superior guidance performance.

REFERENCES

Balakrishnan, S.N. and Biega, V. (1995). A new neural architecture for homeing missile guidance. Proceedings of the 1995 American Control Conference. Seattle Washington USA. 2148-2152.

Chen, Y.W. (2022). Dynamic interception point guidance algorithm based on particle swarm optimization. *Measurement and Control*. 55 (9-10), 983-995.

Chen, K.Y., Lee, Y.L., Liao, S.J., and Kung, C.C. (2016). The design of particle swarm optimization guidance using a line-of-sight evaluation method. *Computers and Electrical Engineering*. 54, 159-169.

Dalton, J. and Balakrishnan, S.N. (1996). A neighboring optimal adaptive critic for missile guidance. *Mathematical and Computer Modelling*. 23 (1-2), 175-188.

Eberhart, R. and Kennedy, J. (1995). A new optimizer using particle swarm theory. Proceedings of the Sixth International Symposium on Micro Machine and Human Science. Nagoya Japan, 39-43.

Fumiaki, I. (1993). Some aspects of a realistic three-dimensional pursuit-evasion game. *Journal of Guidance, Control, and Dynamics*. 16 (2), 289-293.

Kennedy, J. and Eberhart, R. (1995). Particle swarm optimization. Proceedings of the IEEE International Conference on Neural Networks. 4, 1942-1948.

Kung, C.C. and Chen, K.Y. (2013). Missile guidance algorithm design using particle swarm optimization. *Transactions of the Canadian Society for Mechanical Engineering*. 37 (3), 971-979.

Lin, Y.P., Tsao, L.P., and Lin, C.L. (2010). Development of three-dimensional aiming point guidance law. *International Journal of System Science*. 41 (11), 1353-1362.

Mishra, S.K., Sarma, I.G., and Swamy, K.N. (1994). Performance evaluation of two fuzzy-logic-based homing guidance schemes. *Journal of Guidance, Control, and Dynamics*. 17 (6), 1389-1391.

Omar, H.M. and Abido, M.A. (2010). Designing integrated guidance law for aerodynamic missiles by hybrid multi-objective evolutionary algorithm and tabu search. *Aerospace Science and Technology*. 14 (5), 356-363.

Qi, Z.Q., Hu, G.D., Yang, Z.H., and Zhang, F.E. (2003). Flight guidance control using genetic algorithm combined with singular perturbation technique. Proceedings of the Second International Conference on Machine Learning and Cybernetics. Xi'an China, 1034-1038.

Steck, J.E. and Balakrishnan, S.N. (1994). Use of hopfield neural networks in optimal guidance. *IEEE Transactions on Aerospace and Electronic Systems*. 30 (1), 287-293.

Song, E.J. and Tahk, M.J. (1998). Real-time midcourse guidance with intercept point prediction. *Control Engineering Practice*. 6 (8), 957-967.

Song, E.J. and Tahk, M.J. (1999). Real-time midcourse missile guidance robust against launch conditions. *Control Engineering Practice*. 7 (4), 507-515.

Song, E.J. and Tahk, M.J. (2001). Real-time neural-network midcourse guidance. *Control Engineering Practice*. 9 (10), 1145-1154.

Song, E.J. and Tahk, M.J. (2002). Three-dimensional midcourse guidance using neural network for interception of ballistic targets. *IEEE Transactions on Aerospace and Electronic Systems*. 38 (2), 404-414.

Sun, T.Y., Tsai, S.J., and Huo, C.L. (2008). Intelligent maneuvering decision system for computer generated forces using predictive fuzzy inference system. *Journal of Computers*. 3 (11), 58-66.

Siouris, G.M. (2004). Missile Guidance and Control System, Springer. New York.

Wang, Q., Liao, Z. (2024). Computational intelligence interception guidance law using online off-policy integral reinforcement learning. *Journal of Systems Engineering and Electronics*. 35 (4), 1042-1052.

Yang, Z.H., Fang, J.C., and Qi, Z.Q. (2005). Flight midcourse guidance control based on genetic algorithm, Proceedings of the 7th Annual Conference on Genetic and Evolutionary Computation. Washington DC USA, 1501-1506.